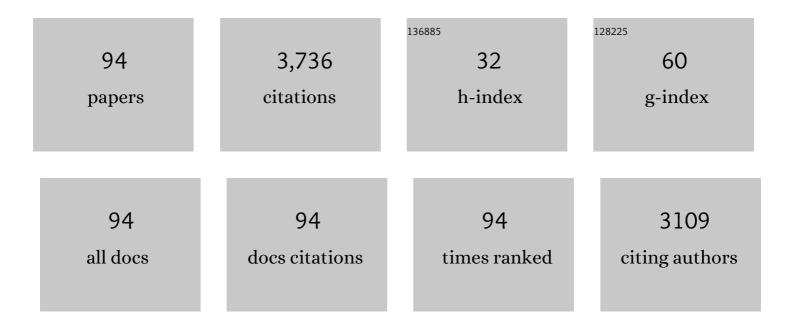
## Scott C Davis

List of Publications by Year in descending order

Source: https://exaly.com/author-pdf/12144805/publications.pdf Version: 2024-02-01



| #  | Article   | IF  | CITATIONS |
|----|---|-----|-----------|
| 1  | Whole-brain MR-registered cryo-imaging of a porcine-human glioma model to compare contrast agent biodistributions. , 2022, , .  |     | 0         |
| 2  | A method for validating depth-resolved biodistributions in topically-stained specimen with multi-channel fluorescence cryo-imaging. , 2021, 11625, .  |     | 0         |
| 3  | A hyperspectral approach for recovering agent excretion biodistributions using whole-body fluorescence cryo-imaging. , 2021, 11625, .   |     | 1         |
| 4  | Clinically relevant dual probe difference specimen imaging (DDSI) protocol for freshly resected breast cancer specimen staining. BMC Cancer, 2021, 21, 440.   | 1.1 | 3         |
| 5  | Examining the Feasibility of Quantifying Receptor Availability Using Cross-Modality Paired-Agent<br>Imaging. Molecular Imaging and Biology, 2021, , 1.  | 1.3 | 0         |
| 6  | Hyperspectral imaging and spectral unmixing for improving whole-body fluorescence cryo-imaging.<br>Biomedical Optics Express, 2021, 12, 395.  | 1.5 | 16        |
| 7  | Monitoring cancer cell surface receptor expression during anti-angiogenesis therapy in vivo.<br>Proceedings of SPIE, 2021, 11625, .   | 0.8 | Ο         |
| 8  | Probeâ€based fluorescence dosimetry of an antibodyâ€dye conjugate to identify head and neck cancer as a<br>first step to fluorescenceâ€guided tissue preselection for pathological assessment. Head and Neck,<br>2020, 42, 59-66. | 0.9 | 7         |
| 9  | Noninvasive quantification of target availability during therapy using paired-agent fluorescence tomography. Theranostics, 2020, 10, 11230-11243.   | 4.6 | 8         |
| 10 | Prediction of optimal contrast times post-imaging agent administration to inform personalized fluorescence-guided surgery. Journal of Biomedical Optics, 2020, 25, .  | 1.4 | 8         |
| 11 | Heterogeneity of circulating tumor cell dissemination and lung metastases in a subcutaneous Lewis<br>lung carcinoma model. Biomedical Optics Express, 2020, 11, 3633.   | 1.5 | 18        |
| 12 | A paired-agent fluorescent molecular imaging strategy for quantifying antibody drug target engagement in in vivo window chamber xenograft models. , 2020, 11219, .  |     | 1         |
| 13 | Estimating drug delivery using hybrid system for simultaneous dynamic MRI and fluorescence tomography. , 2020, 11219, .   |     | Ο         |
| 14 | Developing a novel hyperspectral imaging cryomacrotome for whole body fluorescence imaging. ,<br>2020, 11219, .   |     | 1         |
| 15 | Estimating paired-agent uptake in altered tumor vasculature using MRI-coupled fluorescence tomography. , 2020, 11216, .   |     | 1         |
| 16 | Diagnostic performance of receptor-specific surgical specimen staining correlates with receptor expression level. Journal of Biomedical Optics, 2019, 24, 1.  | 1.4 | 12        |
| 17 | Characterizing short-wave infrared fluorescence of conventional near-infrared fluorophores.<br>Journal of Biomedical Optics, 2019, 24, 1.   | 1.4 | 8         |
| 18 | First experience imaging short-wave infrared fluorescence in a large animal: indocyanine green angiography of a pig brain. Journal of Biomedical Optics, 2019, 24, 1.   | 1.4 | 16        |

| #  | Article  | IF   | CITATIONS |
|----|--|------|-----------|
| 19 | Effect of staining temperature on topical dual stain imaging of tissue specimens for tumor identification. , 2019, 10862, .  |      | 2         |
| 20 | On the use of fluorescein-based contrast agents as analogs to MRI-gadolinium agents for imaging brain tumors. , 2019, 10862, .   |      | 1         |
| 21 | Uptake of a fluorescence imaging agent in an orthotopic glioblastoma using fluorescence molecular tomography. , 2019, , .  |      | Ο         |
| 22 | Noninvasive imaging of dual-agent uptake in glioma and normal tissue using MRI-coupled fluorescence tomography. , 2019, 10874, .   |      | 2         |
| 23 | Diagnostic performance of receptor-specific surgical specimen staining correlate with receptor expression level. , 2019, 10862, .  |      | 0         |
| 24 | Maps of in vivo oxygen pressure with submillimetre resolution and nanomolar sensitivity enabled by<br>Cherenkov-excited luminescence scanned imaging. Nature Biomedical Engineering, 2018, 2, 254-264.                       | 11.6 | 55        |
| 25 | 5-Fluorouracil Enhances Protoporphyrin IX Accumulation and Lesion Clearance during Photodynamic<br>Therapy of Actinic Keratoses: A Mechanism-Based Clinical Trial. Clinical Cancer Research, 2018, 24,<br>3026-3035.         | 3.2  | 38        |
| 26 | Observation of short wavelength infrared (SWIR) Cherenkov emission. Optics Letters, 2018, 43, 3854.  | 1.7  | 17        |
| 27 | Correcting for targeted and control agent signal differences in paired-agent molecular imaging of cancer cell-surface receptors. Journal of Biomedical Optics, 2018, 23, 1.  | 1.4  | 5         |
| 28 | Cherenkov excited short-wavelength infrared fluorescence imaging in vivo with external beam radiation. Journal of Biomedical Optics, 2018, 24, 1.  | 1.4  | 11        |
| 29 | Quantifying cancer cell receptors with paired-agent fluorescent imaging: a novel method to account for tissue optical property effects. , 2018, 10497, .   |      | 1         |
| 30 | Cherenkov-excited luminescence sheet imaging (CELSI) tomographic reconstruction. , 2017, , .   |      | 2         |
| 31 | Assessing daylight & low-dose rate photodynamic therapy efficacy, using biomarkers of<br>photophysical, biochemical and biological damage metrics in situ. Photodiagnosis and Photodynamic<br>Therapy, 2017, 20, 227-233.    | 1.3  | 11        |
| 32 | Simultaneous <i>In Vivo</i> Fluorescent Markers for Perfusion, Protoporphyrin Metabolism, and<br>EGFR Expression for Optically Guided Identification of Orthotopic Glioma. Clinical Cancer Research,<br>2017, 23, 2203-2212. | 3.2  | 36        |
| 33 | Optimization of fluorescent imaging in the operating room through pulsed acquisition and gating to ambient background cycling. Biomedical Optics Express, 2017, 8, 2635.   | 1.5  | 17        |
| 34 | Optimizing fresh specimen staining for rapid identification of tumor biomarkers during surgery.<br>Theranostics, 2017, 7, 4722-4734.   | 4.6  | 21        |
| 35 | Revisiting photodynamic therapy dosimetry: reductionist & surrogate approaches to facilitate clinical success. Physics in Medicine and Biology, 2016, 61, R57-R89.   | 1.6  | 95        |
| 36 | Comparing desferrioxamine and light fractionation enhancement of ALA-PpIX photodynamic therapy in skin cancer. British Journal of Cancer, 2016, 115, 805-813.  | 2.9  | 40        |

| #  | Article   | IF  | CITATIONS |
|----|---|-----|-----------|
| 37 | Small-Animal Imaging Using Diffuse Fluorescence Tomography. Methods in Molecular Biology, 2016, 1444, 123-137.  | 0.4 | 3         |
| 38 | Characterization and standardization of tissue-simulating protoporphyrin IX optical phantoms.<br>Journal of Biomedical Optics, 2016, 21, 035003.  | 1.4 | 25        |
| 39 | Image-derived arterial input function for quantitative fluorescence imaging of receptor-drug binding <i>in vivo</i> . Journal of Biophotonics, 2016, 9, 282-295.  | 1.1 | 7         |
| 40 | Mathematical model to interpret localized reflectance spectra measured in the presence of a strong fluorescence marker. Journal of Biomedical Optics, 2016, 21, 061004.   | 1.4 | 1         |
| 41 | Review of fluorescence guided surgery visualization and overlay techniques. Biomedical Optics<br>Express, 2015, 6, 3765.  | 1.5 | 49        |
| 42 | Noninvasive Optical Imaging of <scp>UV</scp> â€Induced Squamous Cell Carcinoma in Murine Skin:<br>Studies of Early Tumor Development and Vitamin D Enhancement of Protoporphyrin <scp>IX</scp><br>Production. Photochemistry and Photobiology, 2015, 91, 1469-1478. | 1.3 | 16        |
| 43 | Tomography of epidermal growth factor receptor binding to fluorescent Affibody <i>in<br/>vivo</i> studied with magnetic resonance guided fluorescence recovery in varying orthotopic glioma<br>sizes. Journal of Biomedical Optics, 2015, 20, 026001.               | 1.4 | 18        |
| 44 | Video-rate optical dosimetry and dynamic visualization of IMRT and VMAT treatment plans in water using Cherenkov radiation. Medical Physics, 2014, 41, 062102.  | 1.6 | 39        |
| 45 | Dual-channel red/blue fluorescence dosimetry with broadband reflectance spectroscopic correction<br>measures protoporphyrin IX production during photodynamic therapy of actinic keratosis. Journal of<br>Biomedical Optics, 2014, 19, 075002.                      | 1.4 | 45        |
| 46 | Projection imaging of photon beams by the ÄŒerenkov effect. Medical Physics, 2013, 40, 012101.  | 1.6 | 90        |
| 47 | Dual-tracer background subtraction approach for fluorescent molecular tomography. Journal of<br>Biomedical Optics, 2013, 18, 016003.  | 1.4 | 28        |
| 48 | Topical dual-stain difference imaging for rapid intra-operative tumor identification in fresh specimens. Optics Letters, 2013, 38, 5184.  | 1.7 | 29        |
| 49 | Pulsed-light imaging for fluorescence guided surgery under normal room lighting. Optics Letters, 2013, 38, 3249.  | 1.7 | 44        |
| 50 | Three-dimensional ÄŒerenkov tomography of energy deposition from ionizing radiation beams. Optics<br>Letters, 2013, 38, 634.  | 1.7 | 81        |
| 51 | ÄŒerenkov excited fluorescence tomography using external beam radiation. Optics Letters, 2013, 38, 1364.  | 1.7 | 38        |
| 52 | Oxygen tomography by ÄŒerenkov-excited phosphorescence during external beam irradiation. Journal of<br>Biomedical Optics, 2013, 18, 050503.   | 1.4 | 34        |
| 53 | Projection imaging of photon beams using ÄŒerenkov-excited fluorescence. Physics in Medicine and<br>Biology, 2013, 58, 601-619.   | 1.6 | 79        |
| 54 | Fast segmentation and high-quality three-dimensional volume mesh creation from medical images for diffuse optical tomography. Journal of Biomedical Optics, 2013, 18, 086007.   | 1.4 | 151       |

| #  | Article  | IF  | CITATIONS |
|----|--|-----|-----------|
| 55 | Techniques for fluorescence detection of protoporphyrin IX in skin cancers associated with photodynamic therapy. Photonics & Lasers in Medicine, 2013, 2, 287-303.   | 0.3 | 57        |
| 56 | Dynamic dual-tracer MRI-guided fluorescence tomography to quantify receptor density in vivo.<br>Proceedings of the National Academy of Sciences of the United States of America, 2013, 110, 9025-9030.                                       | 3.3 | 89        |
| 57 | White light-informed optical properties improve ultrasound-guided fluorescence tomography of photoactive protoporphyrin IX. Journal of Biomedical Optics, 2013, 18, 046008.  | 1.4 | 19        |
| 58 | An ultrasound-guided fluorescence tomography system: design and specification. , 2013, , .   |     | 0         |
| 59 | Multichannel diffuse optical Raman tomography for bone characterization in vivo: a phantom study.<br>Biomedical Optics Express, 2012, 3, 2299.   | 1.5 | 35        |
| 60 | ÄŒerenkov radiation emission and excited luminescence (CREL) sensitivity during external beam radiation<br>therapy: Monte Carlo and tissue oxygenation phantom studies. Biomedical Optics Express, 2012, 3, 2381.                            | 1.5 | 42        |
| 61 | Time-gated Cherenkov emission spectroscopy from linear accelerator irradiation of tissue phantoms.<br>Optics Letters, 2012, 37, 1193.  | 1.7 | 74        |
| 62 | Double-excitation fluorescence spectral imaging: eliminating tissue auto-fluorescence from<br><i>in vivo</i> PPIX measurements. Proceedings of SPIE, 2012, , .   | 0.8 | 0         |
| 63 | High Vascular Delivery of EGF, but Low Receptor Binding Rate Is Observed in AsPC-1 Tumors as<br>Compared to Normal Pancreas. Molecular Imaging and Biology, 2012, 14, 472-479.   | 1.3 | 31        |
| 64 | Time-gated Cherenkov emission spectroscopy from linear accelerator irradiation of tissue phantoms. , 2012, , .   |     | 4         |
| 65 | Cerenkov emission induced by external beam radiation stimulates molecular fluorescence. Medical Physics, 2011, 38, 4127-4132.  | 1.6 | 92        |
| 66 | MR-GUIDED PULSE OXIMETRY IMAGING OF BREAST IN VIVO. Journal of Innovative Optical Health Sciences, 2011, 04, 199-208.  | 0.5 | 1         |
| 67 | Implicit and explicit prior information in near-infrared spectral imaging: accuracy, quantification and<br>diagnostic value. Philosophical Transactions Series A, Mathematical, Physical, and Engineering<br>Sciences, 2011, 369, 4531-4557. | 1.6 | 36        |
| 68 | MRI-guided fluorescence tomography of PPIX in the breast: a case study. , 2011, , .  |     | 0         |
| 69 | Quantifying receptor density in vivo using a dual probe approach with fluorescence molecular imaging. , 2011, 7965, .  |     | 3         |
| 70 | EGF targeted fluorescence molecular tomography as a predictor of PDT outcomes in pancreas cancer models. , 2010, , .   |     | 1         |
| 71 | Pre-clinical whole-body fluorescence imaging: Review of instruments, methods and applications.<br>Journal of Photochemistry and Photobiology B: Biology, 2010, 98, 77-94.  | 1.7 | 520       |
| 72 | Comparing implementations of magnetic-resonance-guided fluorescence molecular tomography for diagnostic classification of brain tumors. Journal of Biomedical Optics, 2010, 15, 051602.  | 1.4 | 34        |

| #  | Article   | IF  | CITATIONS |
|----|---|-----|-----------|
| 73 | System development for high frequency ultrasound-guided fluorescence quantification of skin<br>layers. Journal of Biomedical Optics, 2010, 15, 026028.  | 1.4 | 24        |
| 74 | MRI-coupled Fluorescence Tomography Quantifies EGFR Activity in Brain Tumors. Academic Radiology, 2010, 17, 271-276.  | 1.3 | 47        |
| 75 | Detecting Epidermal Growth Factor Receptor Tumor Activity In Vivo During Cetuximab Therapy of<br>Murine Gliomas. Academic Radiology, 2010, 17, 7-17.  | 1.3 | 22        |
| 76 | MRI-guided Fluorescence Molecular Tomography to Image Epidermal Growth Factor Receptor Status in<br>Brain Tumors. , 2010, , .   |     | 0         |
| 77 | Spectral distortion in diffuse molecular luminescence tomography in turbid media. Journal of Applied Physics, 2009, 105, 102024.  | 1.1 | 8         |
| 78 | Near infrared optical tomography using NIRFAST: Algorithm for numerical model and image reconstruction. Communications in Numerical Methods in Engineering, 2009, 25, 711-732.                      | 1.3 | 552       |
| 79 | Tissue drug concentration determines whether fluorescence or absorption measurements are more sensitive in diffuse optical tomography of exogenous contrast agents. Applied Optics, 2009, 48, D262. | 2.1 | 8         |
| 80 | Bioluminescence tomography using spectral techniques. , 2009, , .   |     | 0         |
| 81 | MRI-guided fluorescence tomography of the breast: a phantom study. , 2009, , .  |     | Ο         |
| 82 | A study of MRI-guided diffuse fluorescence molecular tomography for monitoring PDT effects in pancreas cancer. , 2009, , .  |     | 4         |
| 83 | Fluorescence tomography characterization for sub-surface imaging with protoporphyrin IX. Optics Express, 2008, 16, 8581.  | 1.7 | 35        |
| 84 | Spectrally resolved bioluminescence tomography using the reciprocity approach. Medical Physics, 2008, 35, 4863-4871.  | 1.6 | 66        |
| 85 | Magnetic resonance–coupled fluorescence tomography scanner for molecular imaging of tissue.<br>Review of Scientific Instruments, 2008, 79, 064302.  | 0.6 | 161       |
| 86 | MRI-coupled spectrally resolved fluorescence tomography for in vivo imaging. , 2008, , .  |     | 2         |
| 87 | System design for spectrally encoded video-rate near infrared tomography during magnetic resonance imaging of the breast. Proceedings of SPIE, 2008, , .  | 0.8 | 0         |
| 88 | MRI-coupled fluorescence tomography of murine glioma metabolic activity. , 2008, , .  |     | 0         |
| 89 | Image Reconstruction in Spectrally Resolved 3D Bioluminescence Tomography using the Adjoint Theorem. , 2008, , .  |     | 1         |
| 90 | Modeling and image reconstruction in spectrally resolved bioluminescence tomography. , 2007, , .  |     | 1         |

| #  | Article  | IF  | CITATIONS |
|----|--|-----|-----------|
| 91 | Image-guided diffuse optical fluorescence tomography implemented with Laplacian-type regularization. Optics Express, 2007, 15, 4066.   | 1.7 | 238       |
| 92 | Subsurface diffuse optical tomography can localize absorber and fluorescent objects but recovered image sensitivity is nonlinear with depth. Applied Optics, 2007, 46, 1669. | 2.1 | 79        |
| 93 | Spectrally resolved bioluminescence optical tomography. Optics Letters, 2006, 31, 365.   | 1.7 | 172       |
| 94 | Contrast-detail analysis characterizing diffuse optical fluorescence tomography image reconstruction. Journal of Biomedical Optics, 2005, 10, 050501.                        | 1.4 | 47        |